Heliyon 7 (2021) e08631

Contents lists available at ScienceDirect

Heliyon

journal homepage: www.cell.com/heliyon

Research article

Multiobjective optimal power flow for static voltage stability margin improvement

Rebeccah Kyomugisha [a,*], Christopher Maina Muriithi [b], Milton Edimu [c]

[a] Electrical Engineering Department, Pan African University Institute for Basic Sciences, Technology and Innovation, Nairobi, Kenya
[b] Electrical Engineering Department, Murang'a University of Technology, Murang'a, Kenya
[c] Electrical and Computer Engineering Department, Makerere University, Kampala, Uganda

ARTICLE INFO

Keywords:
Fuzzy decision making
MOPSO
Preference Selection Index
PV curves
VCPI
Voltage collapse

ABSTRACT

Worldwide, utilities are aiming to increase the stability of modern power systems during system disturbances. Optimizing generation scheduling can improve system security in contingency and stressed conditions while lowering losses and generation costs. An efficient operating strategy for maintaining power system stability is proposed in this work. The paper focuses on incorporating a Voltage Collapse Proximity Index (VCPI) in the traditional optimal power flow problem for multiobjective optimization (MO). Different case studies are assessed to evaluate the impact on the control variables. A Preference Selection index (PSI) is utilized to determine the best-case study for optimal system operation. The effectiveness of the proposed approach is tested on standard IEEE 30-bus and IEEE 57-bus during normal, contingency, and stressed conditions using MATPOWER. During normal conditions, the MO voltage stability constrained optimal power flow (VSC-OPF) increases the system stability by 28.13 % higher than the single objective (SO) case. Furthermore, the transmission losses are lowered by 14.69% with the proposed MO approach. During line outage contingency conditions, the voltage stability enhancement and loss reduction are higher in the MO than in the SO case by 13.60% and 23.19%. However, the loss minimization and stability improvement during normal and contingency conditions come at a slightly higher generation cost of 5.05% in both systems. On the other hand, during stressed conditions, the SO performs better in voltage stability improvement (by 8.77%) and loss reduction (by 6.97%) than in the MO voltage stability constrained OPF. Additionally, PV Curve analysis for the two systems indicates that voltage stability in MO OPF problems provides a more significant margin enhancement of 9.00%, 118.95% in normal and contingency, respectively, higher than the SO case. However, the SO case increases the load margin by 12.36% more than the MO case in stressed conditions. Consequently, the PSI ranks the multiobjective optimization of the three objectives as the most optimal way for operating the systems in normal and line outage contingency conditions. However, during increased load conditions, the system performance is better if a singular objective function is considered. This is due to the lack of adequate reactive power generation during stressed conditions, and hence a singular objective focus is sufficient to assure system stability. Therefore, the proposed approach is an effective preventive control measure for possible voltage collapse in typical power systems. The resulting improvement also brings about a sufficient system stability margin, causing the system to become more secure.

1. Introduction

The voltage instability problem is becoming a severe issue in modern power systems because the generation and transmission capacity is unable to meet the increasing load demand. At the same time, the lack of adequate reactive power sources in the system leads to bulk power losses in transmission lines [1]. The conditions worsen during system disturbances. Therefore, it is essential to consider voltage stability improvement among the objectives of the optimal power flow (OPF) problem. OPF is one of the significant tools used over decades in energy management systems for reliable operation and proper planning of modern power systems. The OPF problem is a non-linear, non-convex, and multi-dimensional optimization problem with control variables such as voltage magnitude, active and reactive power generation as continuous variables, and transformer tap ratios and shunt capacitor as discrete variables [2]. In high-risk voltage instability situations such as heavily

* Corresponding author.
E-mail address: beckykyomugisha@gmail.com (R. Kyomugisha).

https://doi.org/10.1016/j.heliyon.2021.e08631
Received 10 September 2021; Received in revised form 23 October 2021; Accepted 15 December 2021

loaded and line outage contingency conditions, the voltage limit constraint might be insufficient to assure the acceptable voltage stability level. Instead, the objective function should incorporate or focus on the voltage stability enhancement to guarantee system security [3]. Hence, the renewed interest in voltage stability constrained optimal power flow problems [1, 3, 4, 5, 6, 7, 8, 9].

In the recent literature, three main approaches have been used to evaluate the voltage stability constrained OPF (VSC-OPF) problems. Firstly, in [1, 3, 10, 11, 12, 13, 14], the voltage stability indices (VSI) are formulated as singular objective functions. VSIs describe the system stability by measuring the distance of the actual state of the system to the stability limit. In [1], the proposed approach enhanced the voltage stability margin by 19.96%, 7.55%, and 0.18% for IEEE 30-, IEEE 57-, and IEEE 118-bus systems, respectively. Moreover, during line outage conditions, the system loadability was also enhanced by an average of 3.75% across the three test systems. [3] also used this approach to evaluate the effectiveness of different stability indices for generation cost, emission, transmission loss reduction, and maximum loadability enhancement. The results indicated that VCPI reduced the transmission system losses by 58.11%, 49.64%, 35.59% and, 62.00% for IEEE 14-, IEEE 30-, IEEE 57- and IEEE 118-buses, respectively, compared to the L-index. On the other hand, L-index gave the maximum loadability on the test systems. Authors in [5, 15] also incorporated the L-index summation as one of the objective functions for validating the proposed algorithms. In [16], the summation of L-index as the objective function under a single line outage contingency was also evaluated. Despite the simplicity and less computational requirements in this approach [1], there is still a lack of operational practicality. Power systems have conflicting objectives such as generation cost and loss minimization, which must be addressed simultaneously. The generation costs also in this approach are lower since only one objective is minimized. However, the system is more prone to higher transmission losses.

The voltage stability indices are formulated in a multiobjective (MO) optimization problem in the second approach. The MO is treated as a single-objective optimization by assigning suitable weights to each objective function, and then only a single solution is obtained [17, 18]. The merging of voltage stability and generation cost objective functions using the weighted sum approach in [19] provided a higher reduction in generation cost and loss of 0.15% and 7.42%, respectively, compared to the singular objective function approach. Additionally, the voltage stability improvement was 4.03% more than the single-objective approach. However, the problem with this technique is that it requires weights for each objective resulting in the limitation of the available choices and the need for multiple runs [20]. In engineering problems, subjective and unpredictable weightings used in objective functions are the primary cause of a misleading solution because different sensitivities and unpredictable noise of different data sets lead to uncertainty in weighting. Thus, the Pareto optimality approach is an excellent way to obtain a set of possible solutions, including an optimum solution in objective function space, overcoming weighting, and combining [21].

The last approach, the multiobjective optimization method, finds a compromise solution by satisfying two or more objective functions simultaneously. This technique minimizes the voltage stability improvement alongside other competing objectives such as cost and loss minimization. An external repository is utilized to save all non-dominated optimal solutions during the process. Upon having the Pareto-optimal set of non-dominated solutions, a fuzzy decision-making technique is applied to sort out the best compromise solution to the decision-maker. In [4], a multiobjective optimization considering two indices, novel line stability index (NLSI) and critical boundary index (CBI), was performed for stressed system conditions. The analysis revealed that multiobjective VSC-OPF incorporating VSIs enhanced the stability by about 64.558% higher than the single-objective approach [22]. Furthermore, the cost and loss reduction in the VSC-OPF approach [4] was higher by 0.19% and 9.837%, respectively. Authors in [23] also solved a multiobjective OPF of a wind-thermal power system while incorporating the Voltage Stability Enhancement Index (VSEI). The addition of a stability index in multiobjective OPF improved the system stability by 20.477% higher than the single objective function problem of VSEI. There is also a cost and loss reduction of 0.32% and 2.59%, respectively, benefited from using the multiobjective OPF involving the addition of the VSEI. [24, 25] also implemented a multiobjective optimization using the L-index on the IEEE 30- and IEEE 57-bus systems. However, the analyses do not consider any change in the system operating conditions. The studies in this approach demonstrate a significant improvement in the stability and security of the system when VSIs are incorporated in the MO OPF problems. Additional benefits of loss and cost reduction are also achieved with this approach. However, the literature highlighted lacked a holistic justification for using line VSIs in the system. Additionally, no selection mechanism was provided for the different results from the several case studies, leaving the decision prone to human error as operators have to decide the best option for operating the system. This can lead to a compromise of the system's security and stability and eventual system collapse. More so, voltage stability is critical during system disturbances, yet the literature doesn't prioritize system stability improvement during such conditions. As a result, a more detailed analysis is still required to advise utilities on the ideal operating plan.

Therefore, this research proposes an efficient operational strategy for improving static voltage stability during different system conditions. The aim is to justify the significance of multiobjective voltage stability constrained optimization in maintaining system stability during system disturbances. The Multiobjective Particle Swarm Optimisation (MOPSO) algorithm is employed to minimize three objectives of generation cost, transmission loss, and the maximum voltage collapse proximity index (VCPI). To verify the proposed approach, the VSC-OPF is tested on two systems: IEEE 30-bus and IEEE 57-bus systems, under normal, contingency, and stressed operating scenarios. The results from single objective and multiobjective case studies are compared to justify the importance of the approach.

The key contributions of this work are as follows:

(i) Analysis of multiobjective function incorporating the Voltage Collapse Proximity Index for different system operating conditions
(ii) An evaluation of the impact of the system conditions on the static voltage stability performance considering generation cost and power loss
(iii) A ranking of results from the different case studies based on the Preference Selection Index

The advantages of this approach include a fast approximation of distance to collapse due to the use of the superior VCPI index [1, 3, 4] and, it is a time-saving technique for decision-makers as the Preference Selection Index provides a quick output of the best operating case study. However, the challenge remains on the limitation of the generator power outputs that would curtail the level of improvement achieved during system disturbances. Moreover, evaluating two or more objective functions is more complex than one. The proposed approach presented in Figure 1 is applicable in the Energy Control Center as a preventive control measure for possible voltage collapse [1].

The rest of the article is classified into five sections: Section 2 introduces the problem formulation and constraints of the multiobjective optimization problem. Section 3 highlights the basic concepts of multiobjective optimization using the Multiobjective Particle Swarm Optimization Algorithm. Section 4 discusses the optimization results obtained and the system's performance in different operating conditions. Results from five case studies are analyzed here for both IEEE 30- and IEEE 57-bus systems. Finally, in Section 5, the deductions and implications from the simulation findings are presented.

2. Problem formulation

Multiobjective Optimal power flow (MO-OPF) problem is formulated using more than one objective function to find optimal control variables while simultaneously satisfying constraints. This study considers the

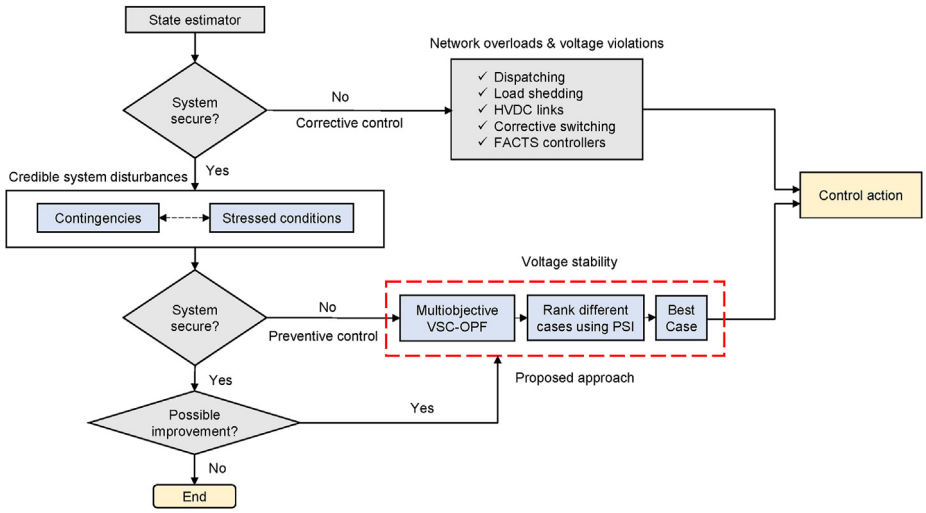

Figure 1. Block schematic of the proposed approach in a typical energy control center (ECC).

minimization of three objective functions; fuel cost, voltage stability, and transmission loss [4]. The general multiobjective approach is formulated with the following primary objective function [26];

$$\text{minimize} \quad f(x) = \left\{f_1(x,u),\, f_2(x,u), f_3(x), \ldots,\, f_{Nobj}(x,u)\right\} \tag{1}$$

subject to

$$g(x,u) = 0 \tag{2}$$

$$h(x,u) \leq 0 \tag{3}$$

where f, g, and h represent the objective function, equality and inequality constraints, respectively. The x vector represents state variables i.e., active power of the slack bus, load bus voltage magnitudes, reactive generator powers, and apparent power flows. x is expressed as in Eq. (4):

$$x = \left[P_{gslack},\ V_{d1}, \ldots,\ V_{dN_d}, Q_{g1},\ \ldots, Q_{gN_s},\ S_{l1},\ \ldots,\ S_{1N_1}\right], \tag{4}$$

where P_{gslack} represents the slack bus generator active power at the slack bus, V_{d1} is the load bus voltage magnitude at bus i, N_g is the total number of generators, S_{li} is the branch i apparent power flow, and N_l is the total number of transmission lines/branches.

u is a vector of control variables consisting of active power generation (except on the slack bus), generator bus voltages, transformer tap ratios, and the reactive powers of shunt compensation capacitors, and is expressed as:

$$u = \left[P_{gi},\ \ldots,\ P_{gN_d}, V_{g1},\ \ldots, V_{gN_s},\ T_1,\ \ldots,\ T_{N_{tran}},\ Q_{c1},\ \ldots,\ Q_{cN_{cap}}\right], \tag{5}$$

Where P_{gi} is the bus i active power generation, V_{gi} is the bus i generator bus voltage magnitude, N_{tran} is the total number of transformer taps, Q_{ci} is the bus i shunt compensation capacitor at i, and N_{cap} is the total number of compensation capacitors.

Multiobjective optimization is a technique built on the principle of Pareto dominance. Details of the Pareto dominance algorithm for optimal solution point sorting can be found in [27]. Figure 2 shows the Pareto optimal solutions based on the concept of nondominated sorting. The Pareto Front (or curve) is a set of nondominated solutions, being chosen as optimal if no objective can be improved without sacrificing at least one other objective.

2.1. Objective functions

In this study, three objective functions of the OPF, consisting of fuel cost, transmission line losses, and maximum value of the line VCPI are considered as detailed below.

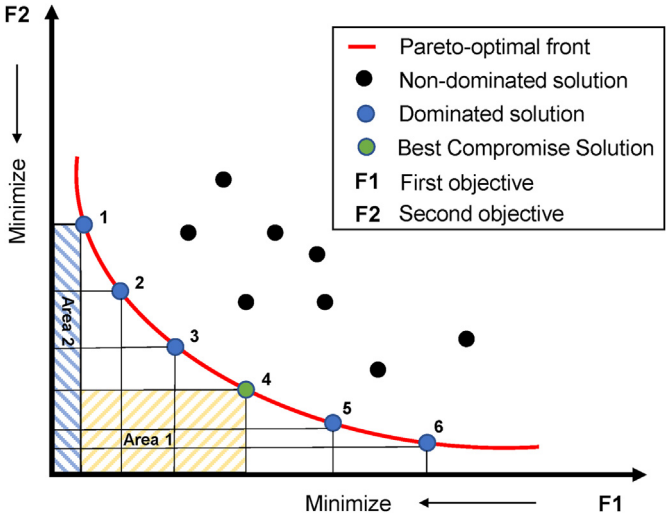

Figure 2. Non-dominated sorting of a population-based on Pareto Front.

2.1.1. Minimization of total fuel cost of generation

The objective here is to minimize the total fuel generation cost. The function is formulated as follows;

$$f_1(x,u) = \sum_{i=1}^{n_g}\left(a_i + b_i P_{g_i} + b_i P_{g_i}^2\right) \tag{6}$$

where $f_c(x)$ is the total fuel cost, n_g is the number of generator buses; a_i, b_i and c_i are the i^{th} generator cost coefficients; and P_{gi} is the active power injection of the i^{th} generator.

2.1.2. Minimization of loss

The objective of this function is to minimize transmission loss in MW. It is given by;

$$f_2(x,u) = \sum_{k=1}^{N_{line}} G_k\left(V_i^2 + V_j^2 - 2V_iV_j\cos\left(\theta_i - \theta_j\right)\right) \tag{7}$$

where G_k is the conductance of the kth line. V_i and V_j are the voltage magnitude at the two ends of line k. θ_i and θ_j are the bus voltage angles at the two ends of line k.

2.1.3. Minimization of the maximum line VCPI

The Voltage Collapse Proximity Index (VCPI) is incorporated into the traditional OPF problem highlighted in Eq. (8). The static voltage stability margin improvement is based on VCPI is proposed as follows;

$$f_3(x,u) = max(VCPI_i) \tag{8}$$

where VCPI is given by [3]:

$$VCPI(power) = \frac{P_r}{P_r(max)} \tag{9}$$

$$P_r(max) = \frac{V_s^2}{Z}\ \frac{cos\varnothing}{4cos^2((\theta-\varnothing)/2)} \tag{10}$$

where $\varnothing = tan^{-1}(Q_r/P_r)$

The value of VCPI increases gradually with increasing power flow through a transmission line. When VCPI reaches the value 1, then voltage collapse occurs. The value of VCPI varies from 0 (no-load condition) to 1 (voltage collapse).

2.2. System constraints

In the OPF problem, there are two types of constraints to consider. Eqs. (11), (12), (13), (14), (15), (16), and (17) describe the system constraints to be handled.

2.2.1. Equality constraints

These include the power balance equations in the network;

$$P_{g_i} - P_{d_i} = V_i \sum_{j=1}^{N} V_j\left(G_{ij}cos\theta_{ij} + B_{ij}sin\theta_{ij}\right) \quad i = 1,\ldots,N \tag{11}$$

$$Q_{g_i} - Q_{d_i} = V_i \sum_{j=1}^{N} V_j\left(G_{ij}sin\theta_{ij} + B_{ij}cos\theta_{ij}\right) \quad i = 1,\ldots,N \tag{12}$$

where P_{gi} and Q_{gi} are the generated active and reactive powers at the i th generator. P_{di} and Q_{gi} are the real and reactive power loads at bus i. V_i and V_j are the voltage magnitude at buses i and j. G_{ij} and B_{ij} denotes line conductance and susceptance between buses i and j, respectively. θ_{ij} is the phase angle difference between buses i and j. N represents the total system buses.

2.2.2. Inequality constraints

The inequality constraints to be considered are as follows:

Generator limits:

$$P_{g_i}^{min} \le P_{g_i} \le P_{g_i}^{max}, \quad i = 1,\ldots,\ N_g \tag{13}$$

$$Q_{g_i}^{min} \le Q_{g_i} \le Q_{g_i}^{max}, \quad i = 1,\ldots,\ N_g \tag{14}$$

$$V_{g_i}^{min} \le V_{g_i} \le V_{g_i}^{max}, \quad i = 1,\ldots,\ N_g \tag{15}$$

Transmission line limits:

$$\left|S_{L_i}\right| \le S_{L_i}^{max}, \tag{16}$$

Load bus voltage magnitude limits:

$$V_{d_i}^{min} \le V_{d_i} \le V_{d_i}^{max}, \quad i = 1,\ldots,N_d \tag{17}$$

where $P_{g_i}^{min}$ is the minimum active power generation, $P_{g_i}^{max}$ the maximum active power generations at bus. $Q_{g_i}^{min}$ and $Q_{g_i}^{max}$ are the minimal and maximum reactive powers generations at bus i. $V_{g_i}^{min}$ and $V_{g_i}^{max}$ are the lower and upper limit of generator voltage magnitudes at bus i. S_{L_i} and $S_{L_i}^{max}$ denote the apparent power flow and its maximum value at branch i. $V_{d_i}^{min}$ and $V_{d_i}^{max}$ are the lower and upper limit load voltages at bus i.

2.3. Constraint handling

Satisfying the equality constraints is guaranteed by running Newton Raphson power flow equations. The inequality constraints are guaranteed through self-restriction of the control variables within predefined boundaries. An extra term called the penalty function that combines all the inequality constraints is added to the primary cost function. In this study, quadratic constraints handling will be used to generate an augmented fitness function of the form [1];

$$J(x,u) = f(x,u) + K_P\left(P_{gslack} - P_{gslack}^{lim}\right)^2 + K_V\sum_{i=1}^{N_{load}}\left(V_{d_i} - V_{d_i}^{lim}\right)^2 + K_Q\sum_{i=1}^{N_{line}}\left(Q_{g_i} - Q_{g_i}^{lim}\right)2 + K_S\sum_{i=1}^{N_{line}}\left(S_{L_i} - S_{L_i}^{lim}\right)^2 \tag{18}$$

where $J(x,u)$ is the penalized objective function; K_p, K_Q, K_V, and K_s are the penalty factors. The original objective function $f(x,u)$ is altered if the solution x is infeasible. P_{gslack}^{lim}, $Q_{g_i}^{lim}$, $V_{d_i}^{lim}$ and $S_{L_i}^{lim}$ are the limit values associated with generator active power, reactive power, load bus voltage, and apparent power. The constraint violations of the state variables are shown in Eqs. (19), (20), (21), and (22).

$$P_{gslack}^{lim} = \begin{cases} P_{gslack}^{max}, & if\ P_{gslack} > P_{gslack}^{max} \\ P_{gslack}, & if\ V_{d_i}^{min} < P_{gslack} < P_{gslack}^{max} \\ P_{gslack}^{min}, & if\ P_{gslack} < P_{gslack}^{min} \end{cases} \tag{19}$$

$$Q_{gi}^{lim} = \begin{cases} Q_{gi}^{max}, & if\ Q_{gi} > Q_{gi}^{max} \\ Q_{gi}, & if\ Q_{gi}^{min} < Q_{gi} < Q_{gi}^{max} \\ Q_{gi}^{min}, & if\ Q_{gi} < Q_{gi}^{min} \end{cases} \tag{20}$$

$$V_{di}^{lim} = \begin{cases} V_{di}^{max}, & if\ V_{di} > V_{di}^{max} \\ V_{di}, & if\ V_{di}^{min} < V_{di} < V_{di}^{max} \\ V_{di}^{min}, & if\ V_{di} < V_{di}^{min} \end{cases} \tag{21}$$

$$S_{L_i}^{lim} = S_{L_i}^{max} \quad if\ S_{Li} > S_{L_i}^{max} \tag{22}$$

The penalty function outputs very high values when the real or active power is outside the allowable range; hence the algorithm moves the active and reactive powers in the permissible limits to avoid a high penalty value.

3. Computational algorithm and procedure

3.1. Multiobjective particle swarm optimization (MOPSO) algorithm

This study's optimization algorithm used to solve the Voltage Stability Constrained OPF is the MOPSO algorithm. It is used to solve the weighting factors problem encountered in PSO by uniting "Pareto-dominance principles" with PSO. The MOPSO approach employed in this work is described in [27, 28]. All of the non-dominated particles in the swarm are gathered into a sub-swarm called Repository, and every particle chooses its global best target among members of this Repository, as highlighted in Figure 3. Like PSO, particles in MOPSO share information and move towards global best particles and their own personal (local) best memory. Using the local best $X_j^*(t)$ and the global best $X_j^{**}(t)$ of each particle,), $j = 1,\ldots,n$, the j^{th} particle velocity in the k^{th} dimension is updated according to Eq. (23). The position is updated according to Eq. (24).

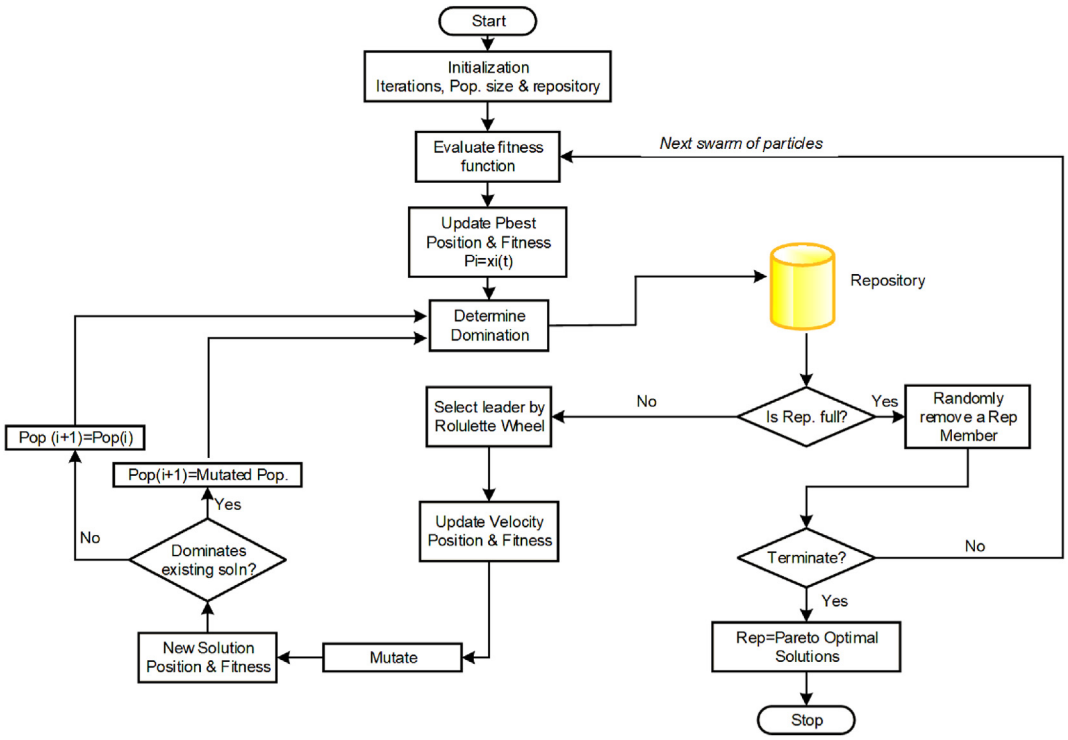

Figure 3. MOPSO algorithm procedure.

$$v_{j,k}(t) = w(t)v_{j,k}(t-1) + c_1 r_1\left(x^{*}_{j,k}(t-1) - x_{j,k}(t-1)\right) + c_2 r_2\left(x^{**}_{j,k}(t-1) - x_{j,k}(t-1)\right) \tag{23}$$

$$x_{j,k}(t) = v_{j,k}(t) + x_{j,k}(t-1) \tag{24}$$

where $v_{j,k}(t)$ represents the velocity of particle j at iteration t. c_1 and c_1 are positive constants and r_1 and r_1 are uniformly distributed random numbers in [0,1]. $x_{j,k}(t)$ is the position of particle j at iteration t.

3.2. Best compromise solution (BCS)

Fuzzy set theory has been commonly used to efficiently choose a candidate Pareto-optimal solution among the many possible solutions on the Pareto front. Due to the nature of the decision maker's irrationality, the $i-th$ objective function of a solution in the Pareto-optimal set, F_i, is represented by a membership function μ_i defined as [29]:

$$\mu_i = \begin{cases} 1, & F_i \le F_i^{min}, \\ \dfrac{F_i^{max} - F_i}{F_i^{max} - F_i^{min}}, & F_i^{min} \le F_i \le F_i^{max}, \\ 0, & F_i \ge F_i^{max} \end{cases} \tag{25}$$

where F_i^{max} and F_i^{min} are maximum and minimum values of the $i-th$ objective function, respectively.

For each non-dominated solution k, the normalized membership function μ^k is calculated as:

$$\mu^k = \frac{\sum_{i=1}^{N_{obj}} \mu_i^k}{\sum_{j=1}^{M}\sum_{i=1}^{N_{obj}} \mu_i^j} \tag{26}$$

The number of nondominated solutions is M. The best compromise solution is the one having the highest value of μ^k. Arranging all solutions in descending order according to their membership function will provide the decision-maker with a priority list of nondominated solutions. This will guide the decision-maker, given the current operating conditions.

4. Results and discussion

The study investigates the system's performance in three operating scenarios when voltage stability is incorporated in the conventional OPF problem. The goal is to improve static voltage stability while meeting other objectives such as generation cost and loss reduction. Two test systems, IEEE 30-bus, and IEEE-57 bus were used to investigate the effectiveness of VSC-OPF on different cases studies of the multiobjective problem. The test system data is detailed as follows:

(i) IEEE 30-bus, shown in Figure 4(a) consists of 30 buses, 6 generators, 41 branches, and 4 transformers. The generators are located at Bus 1, 2, 5, 8, 11, and 13, while transformers are at lines 6–9, 6–10, 4–12, and 27–28. The total connected load is 283.4MW and 126.2MVAR. The detailed data was taken from [30].

(ii) IEEE 57-bus test system includes 57 buses, 7 generators, 80 branches, and 15 transformers. The generators are located at buses 1, 2, 3, 6, 8, 9, and 12. The total active and reactive loads are 1250.8MW and 336.4MVAR, respectively. The data was obtained from [31]. The typical single-line diagram is presented in Figure 4(b).

Tables 1 and 2 show the generator cost functions for IEEE 30-bus and 57-bus respectively.

MATPOWER toolbox in MATLAB was utilized for all power flow and continuation power flow analyses performed in this study. Five case studies were used to evaluate the network's performance under various scenarios. The intention is to demonstrate how the system performs when different generation cost, voltage stability, and loss objectives are considered. The best-case is obtained using the Preference Selection index (PSI). The mathematical formulations of PSI are provided in [32]. The results obtained from Best Compromise Solutions (BCS) obtained under the multiobjective studies are used to further assess the

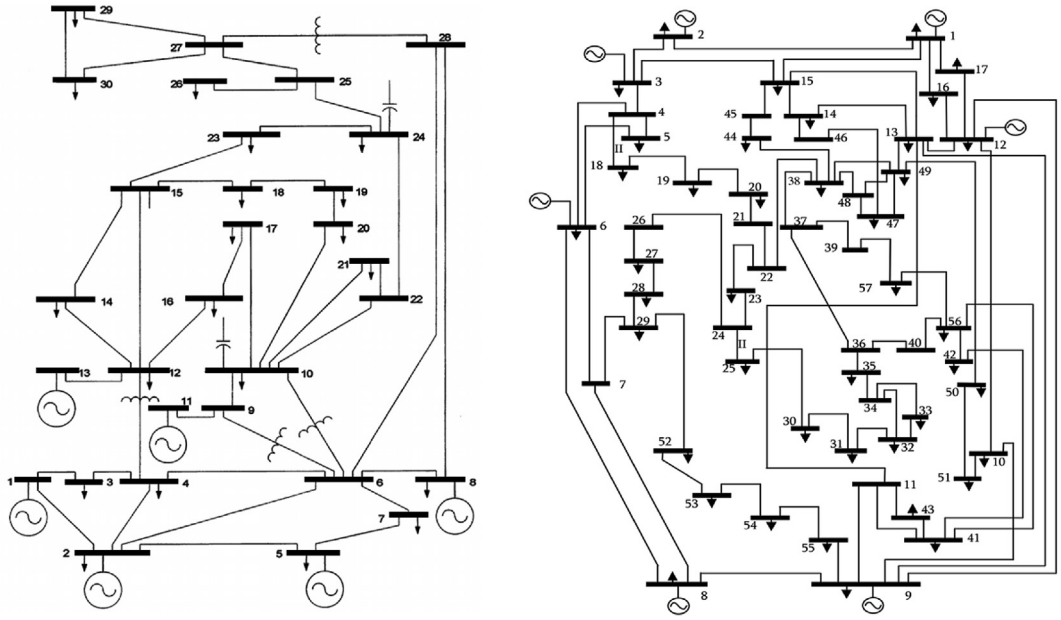

(a) (b)

Figure 4. Single line diagram of the: (a)IEEE 30-bus system (b) IEEE 57-bus system.

Table 1. IEEE 30-bus generator cost coefficients.

Gen	Bus	a	b	c	Pmin	Pmax
1	1	0.00375	2.00	0	50	200
2	2	0.01750	1.75	0	20	80
3	5	0.06250	1.00	0	15	50
4	8	0.00834	3.25	0	10	35
5	11	0.02500	3.00	0	10	30
6	13	0.02500	3.00	0	12	40

Table 2. IEEE 57-bus generator cost coefficients.

Gen	Bus	a	b	c	Pmin	Pmax
1	1	0.0776	20	0	0	575.88
2	2	0.0100	40	0	0	100
3	3	0.2500	20	0	0	140
4	6	0.0100	40	0	0	100
5	8	0.0222	20	0	0	550
6	9	0.0100	40	0	0	100
7	12	0.032258	20	0	0	410

corresponding system voltage, loss, and voltage stability performance. The summary of case studies used in the comparison is as follows:

(i) Base Case: This case evaluates the system when the power outputs are not optimized. The system is operated with active and reactive powers, as presented in Tables 1 and 2.
(ii) Case 0: This case utilizes the inbuilt MATPOWER Interior Point Solver for the optimal power flow problem. It is a single objective optimal power flow considering conventional OPF cost function.
(iii) Case 1: This is a multiobjective optimization considering two objective functions of generation cost and power loss.
(iv) Case 2: This is the second multiobjective problem for two objectives of generation cost and the maximum value of the line Voltage Collapse Proximity Index minimization.
(v) Case 3: This combines all the three objective functions: generation cost, power loss, and the maximum value of the line Voltage Collapse Proximity Index.

The listed case studies were performed for the system in three main operating scenarios described below;

(i) Scenario SC-1: This is the system in normal operating conditions. IEEE 30-bus is operated with load demands of 283.4MW and 126.2MVAR, while IEEE 57-bus has active and reactive loads of 1250.8MW and 336.4MVAR. The total generation is also presented in [30] and [31] for IEEE 30-bus and IEEE 57-bus, respectively.
(ii) Scenario SC-2: This simulates the system in line outage contingency conditions. A ranking of line contingencies based on the line VCPI was performed to simulate this scenario. This is used to identify the system's most critical line. For IEEE 30-bus, Line 1–2, which had the maximum VCPI of 1.3525, was considered for line outage. For the IEEE 57-bus system, Line 8–9 emerged with the maximum VCPI of 1.4989 and therefore, was also considered for line outage.
(iii) Scenario SC-3: This is the system in stressed conditions. Firstly, the maximum loading was obtained for each system using Continuation Power Flow (CPF) analysis. Then, the load demand was increased to close or beyond the normal operating point to simulate the effects of sudden load increase as in the case of faults. The system load on the IEEE 30-bus was increased by 1.4 as indicated in Table 3, similar to [4]. For IEEE 57-bus, the load was increased to 1375.88MW (1.1 times the base load). The purpose was to simulate two systems in which the level of load increase differs and thus, comprehensively evaluate the impact of voltage stability improvement after that.

A summary of all case studies and scenarios considered in this work is presented in Table 3.

The system control variables considered are generator active and reactive power outputs, generator and load bus voltages.

Table 3. Summary of all case studies and scenarios conducted.

Scenarios (SC)	Details		Base	Case 0	Case 1	Case 2	Case 3
IEEE 30-bus							
SC-1: Normal operating conditions	Base load conditions Load demand = 283.4 MW and 126.2 MVAR	Cost	☑	☑	☑	☑	☑
		Loss			☑		☑
		VCPI				☑	☑
SC-2: System under contingency conditions	Maximum VCPI is 1.3525 on Line 1–2. Hence, this line is put out of service	Cost	☑	☑	☑	☑	☑
		Loss			☑		☑
		VCPI				☑	☑
SC-3: System under stressed conditions	Maximum loadability = 1.3057 p.u..p2pLoad demand increased by 1.4 times. New load = 403.8MW and 179.8MVAR	Cost	☑	☑	☑	☑	☑
		Loss			☑		☑
		VCPI				☑	☑
IEEE 57-bus							
SC-1: Normal operating conditions	Base load conditions Load demand = 1250.8MW and 336.4MVAR	Cost	☑	☑	☑	☑	☑
		Loss			☑		☑
		VCPI				☑	☑
SC-2: System under contingency conditions	Maximum VCPI is 1.4989 on Line 8–9. Hence, This line is put out of service	Cost	☑	☑	☑	☑	☑
		Loss			☑		☑
		VCPI				☑	☑
SC-3: System under stressed conditions	Maximum loadability = 0.7153 p.u..p2pLoad demand increased by 1.1 times. New load = 1375.88 MW and 370.04 MVAR	Cost	☑	☑	☑	☑	☑
		Loss			☑		☑
		VCPI				☑	☑

4.1. Multiobjective optimization

This subsection presents the details of the system performance under the multiobjective case studies (Case 1–3) for multiobjective OPF. The Best Compromise Solutions obtained from the pareto fronts have been presented in bold in Tables 4, 6 and 8.

4.1.1. Case 1

In this case, the aim is to minimize two objective functions: generation cost in $/hr. and transmission loss in MW. Figure 5(a) depicts the Pareto optimum solutions for all three scenarios SC-1, SC-2, and SC-3 for the IEEE 30-bus system and Figure 6(a) for the IEEE 57-bus system. Additionally, the BCS from each Pareto group of solutions is highlighted in a red star. As demonstrated in Eqs. (25) and (26), the BCS was derived from the Fuzzy Decision Making (FDM) theory.

The BCS value for SC-1 for IEEE 30-bus was 841.95$/hr for generating cost and 5.54MW for transmission loss. The VCPI(max) stability index for this case was 0.3113, suggesting a steady operating condition. The cost rises to 868.45$/hr since the generation is increased to 292.26MW in contingency conditions (SC-2). The loss and VCPI(max) increase to 8.86MW and 0.7545, respectively, due to an increase in line losses induced by the loss of Line 1–2. However, the system's stability is preserved. The maximum generation costs, losses, and voltage stability index occur when the system is stressed (Cost: 1300.00$/hr, Loss: 15.60MW, and VCPI(max): 1.11). Because 1.11 is over the voltage collapse point of 1, the system may experience voltage collapse under higher load situations. Table 4 shows a comparison of Best Compromise Solutions to the best individual values. As demonstrated in Table 5, the results achieved here are comparable to those published in other recent investigations.

Case 1 of the IEEE 57-bus study shows a similar pattern to the 30-bus. Figure 6(a) demonstrates that when the operating scenario conditions vary from normal (SC-1) to contingency (SC-2) to stressed (SC-3) conditions, the generation cost, power loss, and VCPI(max) all increase. Table 6 summarizes the findings of this Case study. Individual optimization still has the lowest generation cost and loss than multiobjective optimization. The BCS estimates a generating cost of 42,795 dollars per hour and a power loss of 13.37 MW. In SC-1, this corresponds to a VCPI(max) of 0.9997, near the stability limit. As seen in Figure 18, the SC-2 and SC-3 stability limitations are beyond the critical point. Table 7 compares and contrasts the findings of this study with those of prior studies. MOPSO performs comparably to the five other algorithms mentioned.

4.1.2. Case 2

The objective functions in this case study are reduction of generation cost and VCPI(max). All scenarios are considered for analysis for IEEE 30-

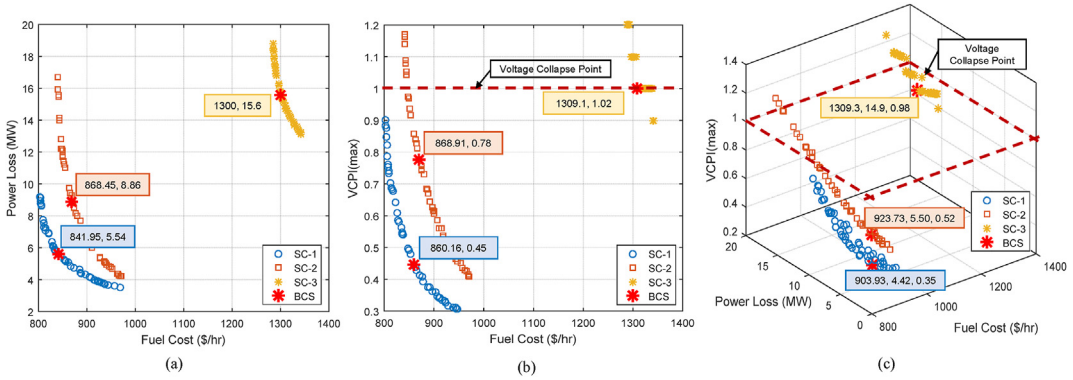

Figure 5. IEEE 30-bus system pareto optimal solutions for: (a) Case 1 (b) Case 2 (c) Case 3.

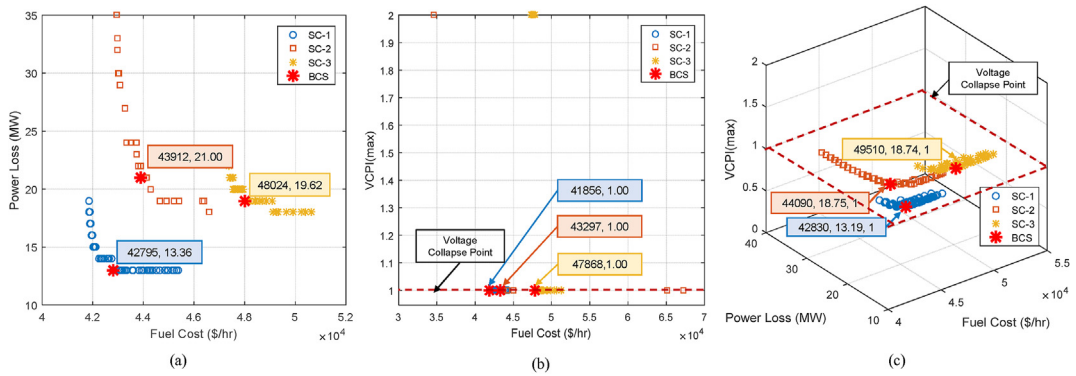

Figure 6. IEEE 57-bus system pareto optimal solutions for: (a) Case 1 (b) Case 2[1] (c) Case 3.[1].

Table 4. IEEE 30-bus summary results for individual best and BCS for Case 1.

Case 1			
Parameter	SC-1	SC-2	SC-3
Individual optimization			
Best Cost ($/hr.)	802.39	840.13	1,285.10
Best Loss (MW)	3.58	4.20	13.10
Best Compromise Solution			
Best Cost ($/hr.)	**841.95**	**868.45**	**1,300.00**
Best Loss (MW)	**5.54**	**8.86**	**15.60**
Pgen (MW)	288.94	292.26	419.15
Qgen (MVAR)	90.13	107.88	183.48
VCPI (max)	0.3113	0.7545	1.1100
VCPI (sum)	4.1512	5.1728	8.1998

Table 5. Comparison of IEEE 30-bus BCS for Case 1 SC-1 results.

Algorithm	Population Size	Iterations	Power Loss (MW)	Fuel Cost ($/h)
MOPSO	50	100	5.5436	841.9512
MOPSO [33]	100	500	4.9785	843.63
PSO [34]	20	200	6.12	850.01
MODA [35]	100	100	4.8143	849.3526
NSGA II [36]	100	300	5.3483	833.5363
MOMICA [37]	120	500	4.5603	848.0544
MOFA-PFA [38]	100	300	4.6727	845.01
MOEA/D [33]	100	500	4.9099	835.36
MOGA [39]	100	300	5.6482	841.05
MOABC/D [40]	100	1000	5.2451	827.636

Table 6. IEEE 57-bus summary results for individual best and BCS for Case 1.

Case 1			
Parameter	SC-1	SC-2	SC-3
Individual optimization			
Best Cost ($/hr.)	41,853.00	42,944.00	47,387
Best Loss (MW)	13.00	18.00	18.00
Best Compromise Solution			
Best Cost ($/hr.)	**42,795.00**	**43,912.00**	**48,024.11**
Best Loss (MW)	**13.37**	**21.00**	**19.62**
Pgen (MW)	1265.17	1265.02	1395.50
Qgen (MVAR)	166.63	176.11	202.26
VCPI (max)	0.9997	1.0339	1.3687
VCPI (sum)	12.7856	12.7281	14.4946

Table 7. Comparison of IEEE 57-bus BCS for Case 1 SC-1 results.

Algorithm	Population Size	Iterations	Power Loss (MW)	Fuel Cost ($/h)
MOPSO	50	100	13.37	42,795
APFPA [41]	30	100	12.1513	43,486
MOCS [42]	100	300	11.99	42,176
MODA [35]	100	300	16.2646	41,903
HFBA-COFS [43]	100	300	10.6995	42,122
NSGA-II [43]	100	500	11.129	42,125
DA [44]	40	300	13.6065	42,584

bus and 57-bus systems, as shown in Figures 5(b) and 6(b). Tables 8 and 10 show the best compromise solutions generated from the Pareto fronts for 30-bus and 57-bus networks, respectively.

When cost and VCPI(max) are considered objective functions, the findings for IEEE 30-bus in Table 8 show a total generation cost of 860.16 $/hr for SC-1, compared to 841.95$/hr for Case 1. The addition of VCPI(max) does not really enhance the system's voltage stability and loss performance.

Table 9 compares the BCS obtained in this work compared to those reported in the literature stated. It can be well observed that L-index provides the lowest values of stability index and highest losses and hence is not efficient in the fast prediction of voltage collapse. VCPI proves to be a superior collapse index.

As shown in Table 10 and Figure 6(b), case 2 performance for IEEE 57-bus results in a compromise generation cost of 41,856 $/hr. for SC-1, 43,297 $/hr. for SC-2, and the highest value of 47,868 $/hr. for SC-3 conditions. The VCPI(max) values are 1.466, 0.860, and 1.745, respectively. Table 10 shows the results for loss performance and comparisons to individual best values. Table 11 compares the results obtained in this study to those obtained in prior studies. The VCPI index continues to indicate an imminent collapse quicker than all other indices, including the LVSI and L-index.

4.1.3. Case 3

Case 3 examines the system's performance while considering all of the generating cost, power loss, and VCPI(max) objectives. Figures 5(c) and 6(c) show the Pareto fronts for the three operational scenarios for IEEE 30- and 57-buses, respectively.

IEEE 30-bus performance under normal operating conditions shows a generating cost of 903.93 $/hr, a power loss of 4.42 $/hr, and a VCPI(-max) of 0.3502. Case 3 findings indicate an increase in generation cost while loss and VCPI(max) decrease in all operating conditions SC-1, SC-2, and SC-3 (see Table 12).

Compared to cases 1 and 2, the tri-objective function for IEEE 57-bus shows a modest rise in cost in SC-1 and SC-2. Opposed to Case 2, the

Table 8. IEEE 30-bus summary results for individual best and BCS for Case 2.

Case 2			
Parameter	SC-1	SC-2	SC-3
Individual optimization			
Best Cost ($/hr.)	802.92	840.65	1,288.30
Best VCPI(max)	0.3058	0.4091	0.9000
Best Compromise Solution			
Best Cost ($/hr.)	**860.16**	**868.91**	**1,309.10**
Best VCPImax	**0.4450**	**0.7774**	**1.0200**
VCPI (sum)	4.7968	5.2159	8.6677
Pgen (MW)	288.93	292.37	421.68
Qgen (MVAR)	90.20	107.98	192.91
Loss (MW)	5.53	8.97	17.88

Table 9. Comparison of IEEE 30-bus BCS for Case 2 SC-1.

Algorithm	Stability Index	Fuel Cost ($/h)	Power Loss (MW)	Max of Index	Sum of Index
MOPSO	VCPI	860.1559	5.53	0.445	4.7968
WEA [45]	L-index	847.331	9.3141	0.1099	-
Mjaya [46]	L-index	801.0117	8.7715	0.12485	-
MSA [24]	L-index	804.4838	9.9486	0.13917	-

Table 10. IEEE 57-bus summary results for individual best and BCS for Case 2.

Case 2			
Parameter	SC-1	SC-2	SC-3
Individual optimization			
Best Cost ($/hr.)	41,738	41,754	47,371
Best VCPI(max)	1.025	0.724	1.365
Best Compromise Solution			
Best Cost ($/hr.)	**41,856.00**	**43,297.01**	**47,868.16**
Best VCPI(max)	**1.4658**	**0.8596**	**1.4229**
VCPI (sum)	13.7839	14.0564	14.6862
Pgen (MW)	1269.61	1271.81	1396.06
Qgen (MVAR)	174.97	190.78	202.77
Loss (MW)	17.61	20.01	20.18

Table 11. Comparison of IEEE 57-bus BCS for Case 2 SC-1.

Algorithm	Stability Index	Fuel Cost ($/h)	Power Loss (MW)	Max of Index	Sum of Index
MOPSO	VCPI	41,856	17.613	1.4658	13.7839
MOPSO [25]	L-index	41,607	13.3730	0.2018	-
Jaya [47]	L-index	43,684	12.912	0.2302	-
DA [44]	L-index	42,584	13.6065	0.2638	-
DA-PSO [1]	LVSI	41,828	16.63	0.8731	13.82

voltage stability improves significantly in Case 3, with the VCPI(max) falling to 0.9965 for SC-1, 0.792 for SC-2, and 1.1285 for SC-3. Case 3 also has the least amount of power loss when contrasted to Cases 1 and 2 (see Table 13).

[1] Please note the VCPI(max) figures were rounded off in the graph due to the 1e4 factor on the x-axis. For actual values, see Tables 6, 10, 13.

Table 12. IEEE 30-bus summary results for individual best and BCS for Case 3.

Case 3			
Parameter	SC-1	SC-2	SC-3
Individual optimization			
Best Cost ($/hr.)	802.96	840.09	1,285.50
Best Loss (MW)	3.51	4.31	13.10
Best VCPI(max)	0.31	0.42	0.90
Best Compromise Solution			
Best Cost ($/hr.)	**903.93**	**923.73**	**1,309.30**
Best Loss (MW)	**4.42**	**5.50**	**14.90**
Best VCPI(max)	**0.3502**	**0.5153**	**0.9840**
VCPI (sum)	4.4019	4.5358	8.0510
Pgen (MW)	287.85	288.90	418.47
Qgen (MVAR)	86.24	96.16	181.02

Table 13. IEEE 57-bus summary results for individual best and BCS for Case 3.

Case 3			
Parameter	SC-1	SC-2	SC-3
Individual optimization			
Best Cost ($/hr.)	41,883.00	42,934.00	47,379
Best Loss (MW)	13.00	18.00	18.00
Best VCPI(max)	0.924	0.644	1.000
Best Compromise Solution			
Best Cost ($/hr.)	**42,830.00**	**46,374.13**	**49,510.29**
Best Loss (MW)	**13.20**	**18.58**	**18.74**
Best VCPI(max)	**0.9970**	**0.7920**	**1.1285**
VCPI (sum)	12.1290	13.2320	14.0734
Pgen (MW)	1265.01	1269.38	1394.62
Qgen (MVAR)	166.31	181.23	197.94

4.2. System performance under different operating conditions

This section includes comparison studies between the case studies for each scenario considered. The purpose is to provide a general contrast in the system's performance when different objectives of generation cost, stability, and loss are considered. The obtained Best Compromise Solutions (BCS) obtained under the multiobjective studies are used to perform further system analyses in this section. For all scenarios, the best case obtained using the PSI has been made bold in Tables 14, 15, 16, 17, 18 and 19.

Contingency conditions alter the system configuration, making it more unstable and insecure. As stated earlier, the contingency ranking was obtained from the maximum value of the line VSI. On the other hand, sudden increased load conditions create stressed system conditions. In such scenarios, the reactive power demand is highest. Consequently, the system is forced to operate close to or beyond stability limits.

4.2.1. Scenario SC-1 (normal operating conditions)

4.2.1.1. IEEE 30-bus. Under this scenario, the system is operated in normal conditions as presented in Table 14 and Figure 7. As expected, the lowest costs (802.20$/hr.) are encountered in the single-objective optimization since only one objective function is minimized. The addition of voltage stability increases costs in Case 2 and 3 since active power outputs from the generators are being increased to ensure system stability. Case 3 costs (903.926 $/hr.) are highest because the highest active power increase of 118.95% (from 11.36MW for Case 0–24.86MW in Case 3) is encountered at bus 13, which is the most expensive generator. Regarding voltage stability, Case 1 encounters the lowest VCPI index of 0.3113, although this comes at a slightly higher power loss. Multiobjective optimization of the three objectives simultaneously offers the most

Table 14. IEEE 30-bus summary results for different case studies under normal conditions (SC-1).

SC-1									
Cases	Total Cost ($/hr.)	Total Pgen (MW)	Total Qgen (MVAR)	Ploss (MW)	Power Loss (%)	VCPI (max)	VCPI (sum)	PSI	Rank
Base	875.283	300.96	133.93	17.56	6.20%	1.3525	7.5736	0.5997	5
Case 0	802.204	292.86	103.98	9.46	3.34%	0.9001	6.0016	0.7316	4
Case 1	841.951	287.18	84.25	5.54	1.96%	0.3113	4.1512	0.9450	2
Case 2	860.156	288.93	90.20	5.53	1.95%	0.4450	4.7968	0.8800	3
Case 3	**903.926**	**287.85**	**86.24**	**4.42**	**1.56%**	**0.3502**	**4.4019**	**0.9562**	**1**

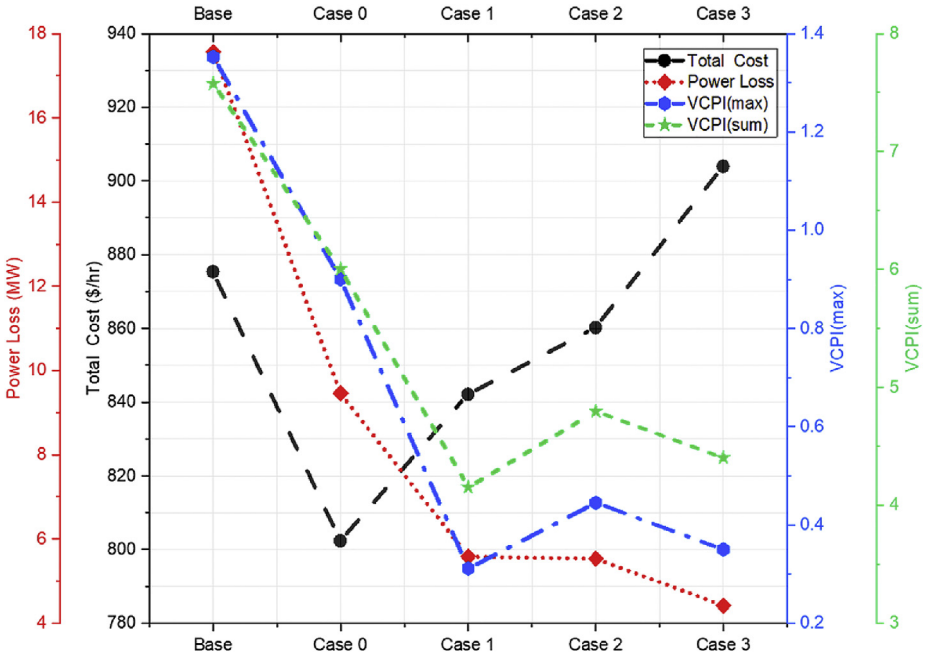

Figure 7. IEEE 30-bus SC-1 summary of system performance.

optimal variable outputs in cost, loss, and voltage stability, hence the highest PSI index of 0.9562.

Using the VSI as a single objective function in [1] yielded a much higher cost of 971.55 $/h compared to the 903.926 $/hr. obtained for the best case in Table 14. Additionally, the power loss obtained in Table 14 (4.42 MW) is still lower than the reported value of 4.7236 MW in [1]. Therefore, multiobjective VSC-OPF has proven more efficient for the system operation of the IEEE 30-bus in normal operating conditions.

4.2.1.2. IEEE 57-bus. A considerable cost reduction of 32.32% is realized when only the generation cost function is minimized as in Case 0, as shown in Table 15 and Figure 8. Voltage stability is compromised in this case, as stability is not a priority in the goals. Thus, in Case 0, the system is doomed to collapse due to the VCPI(max) value of 1.5180, which is more than the collapse point of 1. Case 2, which emphasizes cost and VCPI minimization, is also at risk of collapsing because the system loss, which is not prioritized in the objectives, eventually compromises generator outputs, causing the system to become unstable. Hence its VCPI(max) of 1.4660. However, a stable voltage condition in this system is still realized when the three functions of cost, loss, and voltage stability are all optimized at once. This is illustrated with Case 3, with a voltage stability index of 0.9970. The lowest losses of 13.199MW (1.06%) are still realized with this case study since the loss is also prioritized. Hence, the system outputs are increased to ensure loss minimization and a stable voltage system. Case 3 is the preferred case with the highest PSI of 0.9963.

These results are similar to those obtained in [1], where 44,054.27 $/hr cost. was obtained using the LVSI index. Similarly, the single objective optimization of the LVSI index summation yielded a voltage stability improvement of 7.55% compared to the 34.32% obtained in the multiobjective Case 3 (using Case 0 for comparison). Using the multiobjective optimization also has the advantage of a lower cost of 42, 830.00 $/hr. and power loss of 13.199MW compared to the 13.55MW in [1].

4.2.2. Scenario SC-2 (contingency conditions)

4.2.2.1. IEEE 30-bus. With Line 1–2 out of service on IEEE 30-bus, the generated active power at Generator 1 increases by 16.50% (from 260.96 MW to 304.03MW). The reactive power also generated significantly increases (118.11%) to maintain bus voltages within allowable limits. The losses also significantly increase on Line 1–3 to 37.999 MW from 3.108MW due to overloading caused by loss of Line 1–2. All these factors culminate into an unstable system with the highest costs represented by the Base costs of 1052.68 $/hr., shown in Table 16 and Figure 9. Optimization of these parameters shows that the generator active powers can be minimized to a total generation of 288.9 MW with the lowest loss of 1.94%, as in Case 3. The system is also most stable in this case study, with a VCPI(max) of 0.5153. This implies that multiobjective optimization is significant in preventing possible system collapse under contingency conditions, as can be seen in the low values of VCPI(max) for Cases 1–3. Therefore, multiobjective optimization provides the most balanced

Table 15. IEEE 57-bus summary results for different case studies under normal conditions (SC-1).

SC-1									
Cases	Total Cost ($/hr.)	Total Pgen (MW)	Total Qgen (MVAR)	Ploss (MW)	Ploss (%)	VCPI (max)	VCPI (sum)	PSI	Rank
Base	61667.15	1288.962	253.833	27.864	2.23%	1.4990	16.8340	0.6747	5
Case 0	41737.79	1267.312	227.301	16.512	1.32%	1.5180	13.6890	0.8449	4
Case 1	42795.00	1265.170	166.630	13.365	1.07%	1.0000	12.7860	0.9850	2
Case 2	41856.00	1269.610	174.970	17.613	1.41%	1.4660	13.7840	0.8645	3
Case 3	**42830.00**	**1265.010**	**166.310**	**13.199**	**1.06%**	**0.9970**	**12.1290**	**0.9963**	**1**

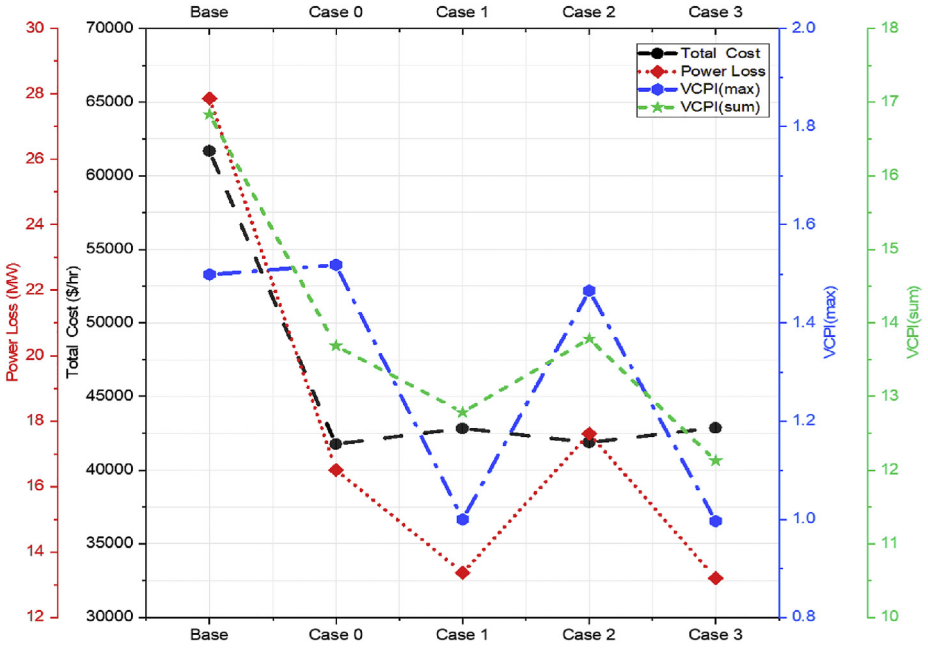

Figure 8. IEEE 57-bus SC-1 summary of system performance.

system operation for the IEEE 30-bus under line outage contingency conditions optimally. This is validated under Case 3, with the highest PSI index of 0.9839.

The optimized values for Case 3 are largely comparable to those obtained by [1]. The cost of 923.73 $/hr. is lower compared to the 972.72 $.hr. obtained in [1]. More so, the loss results in Case 3 (5.50 MW) are still lower than those obtained in the literature stated (5.21 MW). Whereas [1] used the minimization of LVSI sum as the objective function, the tri-objective optimization has proven superior in enhancing system operating conditions while assuring system security.

4.2.2.2. IEEE 57-bus. When Line 8–9 is put out of service for this scenario, the system active power generation increases to 1311.91 MW from 1278.66 MW. The increase mainly occurs at the generator on Bus 1. The reactive power also increases by 35.80% to maintain system bus voltage magnitudes. However, the system losses increase by 119.29% due to the strain imposed on lines 6–8 and 7–8. In these conditions, the system is prone to collapse, as evidenced by the VCPI(max) value of 1.7150, as shown in Table 17. However, optimizing the system parameters in this scenario shows that multiobjective case studies 2 and 3 can maintain system stability, as seen by the lower VCPI(max) values in Figure 10. The system loss can also be significantly reduced to about 1.49%, as realized in Case 3. Even though the highest generation costs are incurred in Case 3, the system can achieve the optimum operating condition in terms of costs, loss, and voltage stability. As such, Case 3 emerges as the best case to operate IEEE 57-bus in contingency conditions, hence the highest PSI of 0.9737. This is similar to the results presented in [1], where a slightly lower cost of 46,415.52 $/hr. was obtained from the minimization of the LVSI sum as the objective function. The losses obtained of 17.63 MW are also slightly lower than those obtained in Table 17. This confirms the robustness of the VCPI index in OPF problems.

Table 16. IEEE 30-bus summary results for different case studies under Contingency Conditions (SC-2).

SC-2									
Cases	Total Cost ($/hr.)	Total Pgen (MW)	Total Qgen (MVAR)	Ploss (MW)	Ploss (%)	VCPI (max)	VCPI (sum)	PSI	Rank
Base	1052.68	344.03	292.11	60.63	21.39%	2.5781	10.4734	0.4602	5
Case 0	843.22	296.15	122.18	12.75	4.50%	1.0317	5.9958	0.7449	4
Case 1	868.45	292.26	107.88	8.86	3.13%	0.7545	5.1728	0.8380	2
Case 2	868.91	292.37	107.98	8.97	3.17%	0.7774	5.2159	0.8325	3
Case 3	**923.73**	**288.90**	**96.16**	**5.50**	**1.94%**	**0.5153**	**4.5358**	**0.9839**	**1**

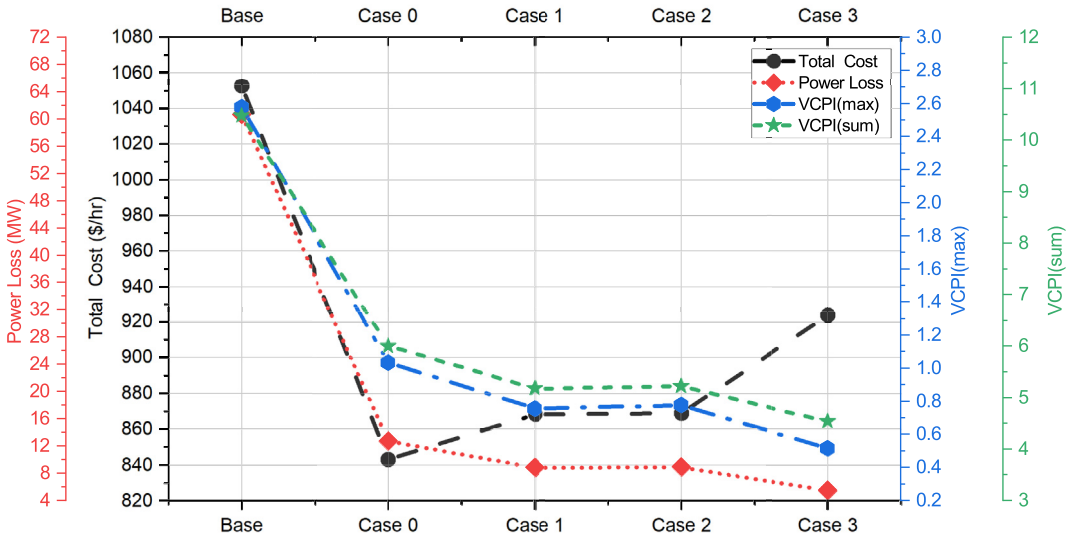

Figure 9. IEEE 30-bus SC-2 summary of system performance.

Table 17. IEEE 57-bus summary results for different case studies under Contingency Conditions (SC-2).

SC-2									
Cases	Total Cost ($/hr.)	Total Pgen (MW)	Total Qgen (MVAR)	Ploss (MW)	Ploss (%)	VCPI (max)	VCPI (sum)	PSI	Rank
Base	42964.86	1264.15	173.55	61.11	4.89%	1.7150	25.1667	0.6993	5
Case 0	42674.33	1281.16	239.11	30.36	2.43%	1.3651	17.0553	0.7738	4
Case 1	43912.00	1265.02	176.11	21.00	1.68%	1.0339	12.7281	0.9356	3
Case 2	43297.01	1271.81	190.78	20.01	1.60%	0.8596	14.0564	0.9423	2
Case 3	**46374.13**	**1269.38**	**181.23**	**18.58**	**1.49%**	**0.7925**	**13.2322**	**0.9737**	**1**

4.2.3. Scenario SC-3 (stressed conditions)

4.2.3.1. IEEE 30-bus. The active power rises to 443.63 MW in this scenario to handle the increased load. The generated reactive power also increases to 273.39 MVAR to provide voltage support to the reactive loads. In these conditions, the power loss is significantly high to about 9.86% due to the high need for reactive power and increased stress on the lines. The optimization of system parameters presented in Table 18 and Figure 11 indicates a significant reduction in generation costs due to optimizing generator active power outputs. The least active and reactive power requirements occur in Case 0. This also translates to the least losses and the most voltage stable condition. Hence, the single optimization case (case 0) is optimal to operate the IEEE 30-bus in stressed conditions. This can be attributed to the fact that the system needs to meet the required demand in such disturbance conditions. Hence utilities ought to focus on increasing the generation and reactive power needs.

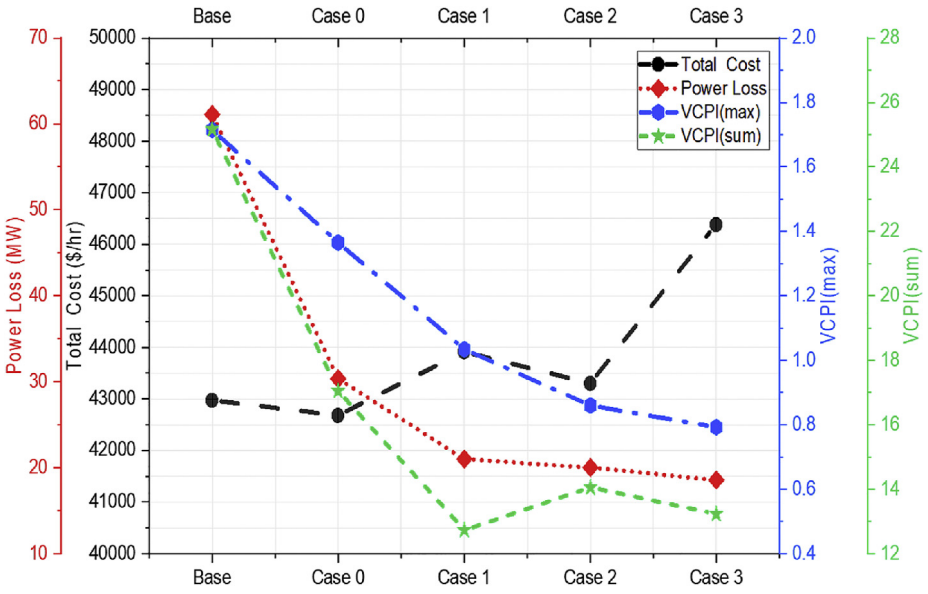

Figure 10. IEEE 57-bus SC-2 summary of system performance.

Table 18. IEEE 30-bus summary results for different case studies under stressed conditions (SC-3).

SC-3									
Cases	Total Cost ($/hr.)	Total Pgen (MW)	Total Qgen (MVAR)	Ploss (MW)	Ploss (%)	VCPI (max)	VCPI (sum)	PSI	Rank
Base	1516.19	443.63	273.39	39.83	9.86%	2.3267	12.1116	0.62129	5
Case 0	**1305.85**	**416.58**	**176.66**	**12.78**	**3.16%**	**0.9822**	**7.8038**	**0.99927**	**1**
Case 1	1300.00	419.15	183.48	15.6	3.86%	1.1100	8.1998	0.92757	3
Case 2	1309.10	421.68	192.91	17.88	4.43%	1.0228	8.6677	0.89459	4
Case 3	1309.30	418.47	181.02	14.9	3.69%	0.9840	8.0510	0.95492	2

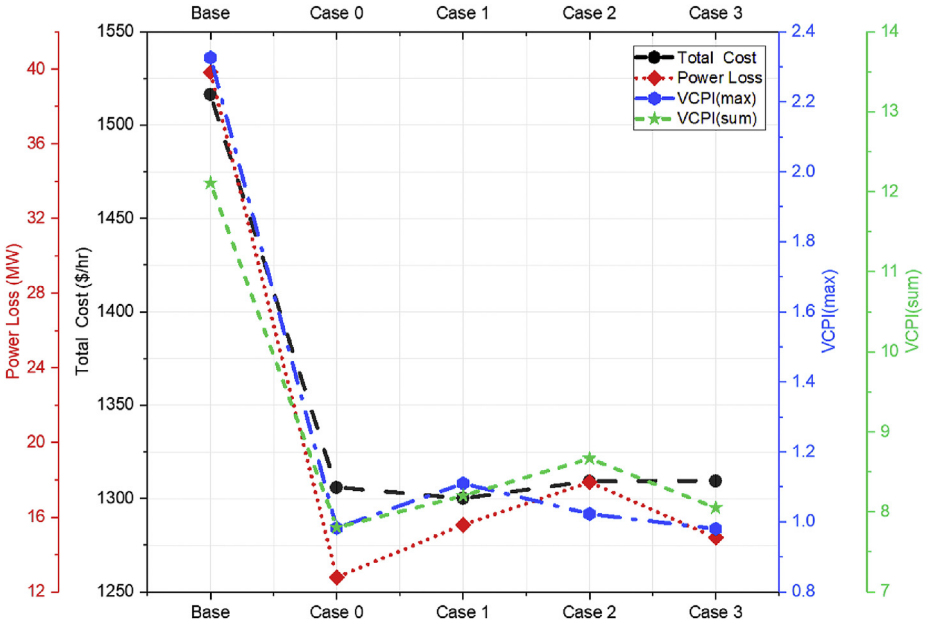

Figure 11. IEEE 30-bus SC-3 summary of system performance.

The voltage stability and loss objectives would be directly enhanced upon matching the supply to the demand.

Consequently, multiobjective optimization may not be a priority when undergoing significant stress. It is important to note that the multiobjective results obtained in this scenario are similar to those obtained by Adewuyi *et al.* in [4]. The IEEE 30-bus assessed in stressed conditions using the Critical Boundary Index (CBI) revealed a total cost of 1310.90 $/hr. for Case 2 comparable to 1309.10$/hr. obtained in Table 18 using VCPI.

4.2.3.2. IEEE 57-bus. The system performance of the IEEE 57-bus in stressed conditions is indicated in Table 19. Figure 12 presents the variable comparisons. Using a factor of 1.1 p.u., the system significantly increased the system load, causing the power generation to increase to 1417.28 MW to meet the increased demand. These conditions also escalate the stress on the lines, increasing the losses by 48.58%. The active power generation is decreased from the base case by 1.96% for Case 0, 1.54% for Case 1, 1.50% for Case 2, and 1.60% for Case 3. All the optimization case studies also minimize transmission losses by 57.80%, 52.61%, 51.25%, and 54.73% lower than the base case for Case 0, Case 1, Case 2, and Case 3, respectively. Moreover, Cases 0, 1, 2, and 3 cost 24.33%, 27.13%, 27.37% and 24.88% lower than the base case, respectively. The VCPI(max) and VCPI(sum) values are also improved with the most voltage stable case in Case 0. According to the PSI ranking (0.9628), the single optimization case (Case 0) gives the best cost, active and reactive power generation, loss, and voltage stability. This is because in stressed conditions, such as fault scenarios, the system's active and reactive power demands are enormous. Therefore, the goal is to try as much as possible to meet the demand. Hence, the priority is the optimization of generator outputs. As in Cases 1–3, the addition of other objective functions does not necessarily improve the system condition.

Table 19. IEEE 57-bus summary results for different case studies under stressed conditions (SC-3).

SC-3									
Cases	Total Cost ($/hr.)	Total Pgen (MW)	Total Qgen (MVAR)	Ploss (MW)	Ploss (%)	VCPI (max)	VCPI (sum)	PSI	Rank
Base	65,906.23	1,417.28	250.49	41.401	3.01%	1.6587	20.5108	0.6747	5
Case 0	**49,873.62**	**1,389.51**	**249.15**	**17.471**	**1.27%**	**1.0000**	**13.8159**	**0.9628**	**1**
Case 1	48,024.11	1,395.50	202.26	19.618	1.43%	1.3687	14.4946	0.9229	3
Case 2	47,868.16	1,396.06	202.77	20.181	1.47%	1.4229	14.6862	0.9109	4
Case 3	49,510.29	1,394.62	197.94	18.742	1.36%	1.1285	14.0734	0.9585	2

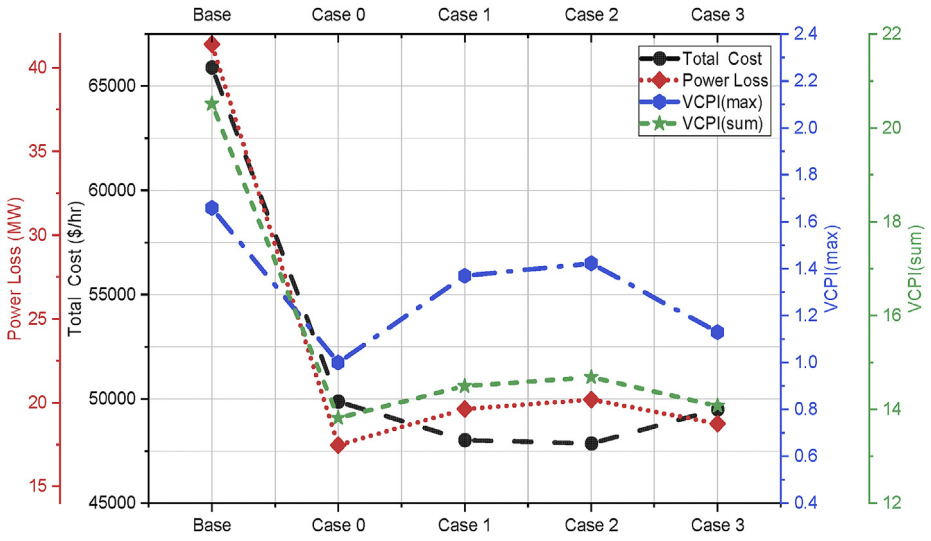

Figure 12. IEEE 57-bus SC-3 summary of system performance.

4.3. Impact on voltage stability

4.3.1. Bus voltage magnitude

It is good to mention that all bus voltage magnitudes are respected in all the scenarios and case studies, as shown in Figures 13, 14. MATPOWER lower and upper limits of 0.94 p.u. and 1.06 p.u. were maintained in all analyses. In normal operating conditions, IEEE 30-bus had the lowest voltage at Bus 30 (weakest bus) at 0.992 p.u. and highest at Bus 11 (1.082 p.u.). All optimization results provided bus voltages within acceptable ranges, as shown in Figure 13, with an average improvement of 0.11%, 0.99%, 0.17% in normal, contingency, and stressed conditions, respectively.

Similarly, for IEEE 57-bus, the lowest bus voltages were obtained at the weakest Bus 31 (0.936 p.u.) and highest at Bus 48 (1.06 p.u.) in normal operating conditions. Bus 31 voltage drops to 0.919 p.u. after the loss of Line 8–9, and to 0.892 p.u. in stressed conditions. Figure 14 shows

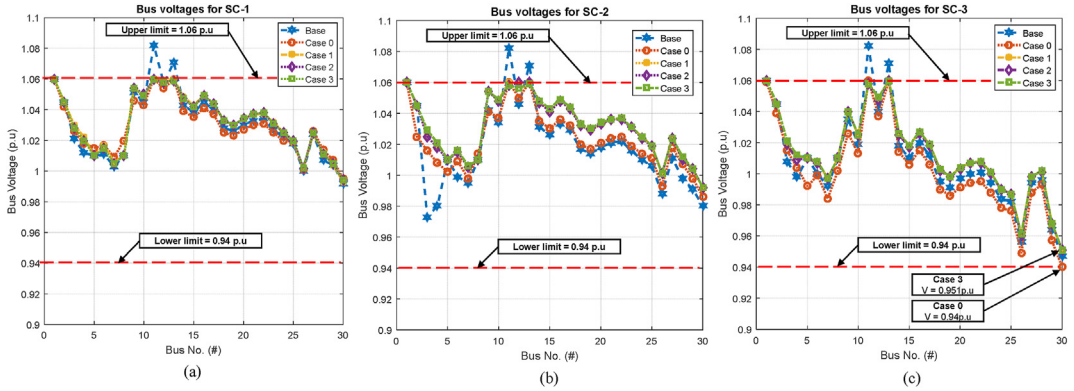

Figure 13. IEEE 30-bus voltage magnitudes for: (a) SC-1 (b) SC-2 (c) SC-3.

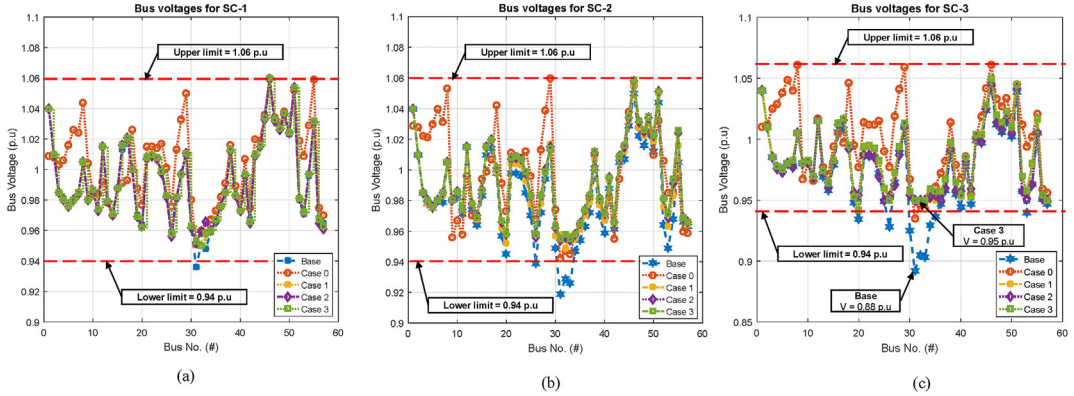

Figure 14. IEEE 57-bus voltage magnitudes for: (a) SC-1 (b) SC-2 (c) SC-3.

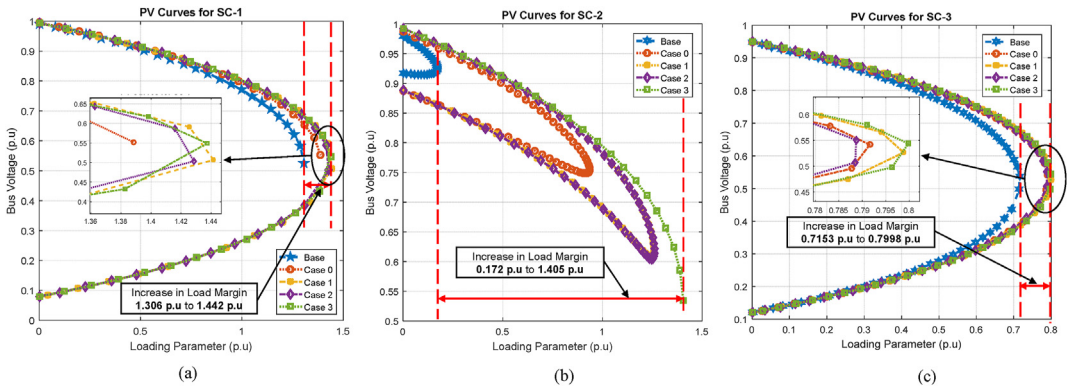

Figure 15. IEEE 30-bus PV Curves for Bus 30 for scenarios: (a) SC-1 (b) SC-2 (c)SC-3.

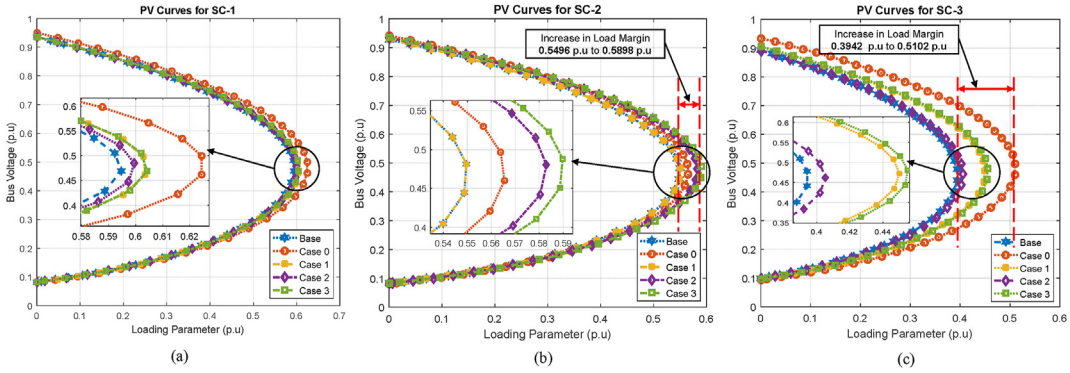

Figure 16. IEEE 57-bus PV Curves for Bus 31 for scenarios: (a) SC-1 (b) SC-2 (c)SC-3.

that an average improvement of 0.330%, 0.992%, and 1.337% is realized in normal, contingency, and stressed conditions, respectively.

4.3.2. Maximum system loadability (PV curves)

The PV curves for the weakest buses all case studies and scenarios are shown in Figures 15 and 16 for IEEE 30-bus and IEEE 57-bus, respectively. In the normal conditions for IEEE 30-bus, Case 1 offers the largest loadability margin improvement of 10.41%, improving the stability margin by 3.56%, hence increasing the system security. During contingency conditions, the system loadability is lowest in the base case (0.172 p.u.). However, an improvement of over 610% is realized on average in all the cases, with the highest occurring in Case 3. The margin of the voltage stability is also improved by an average of 31.58% across Case 0–3. In stressed conditions, significant loadability margin enhancement of 10.67%, 11.67%,10.26%,11.81% for Case 0, Case 1, Case 2 and Case 3 respectively, is also achieved.

For the IEEE 57-bus system, the simulation results indicate a significant improvement in the voltage stability margin. During system disturbances, the system load margin increases up to a maximum of 7.31% (Case 3) and 40.46% (Case 0) for contingency and stressed conditions, respectively. The critical voltage also reduces by 1.42 % (Case 3) during the loss of Line 1–2, making the system more secure and stable for operation.

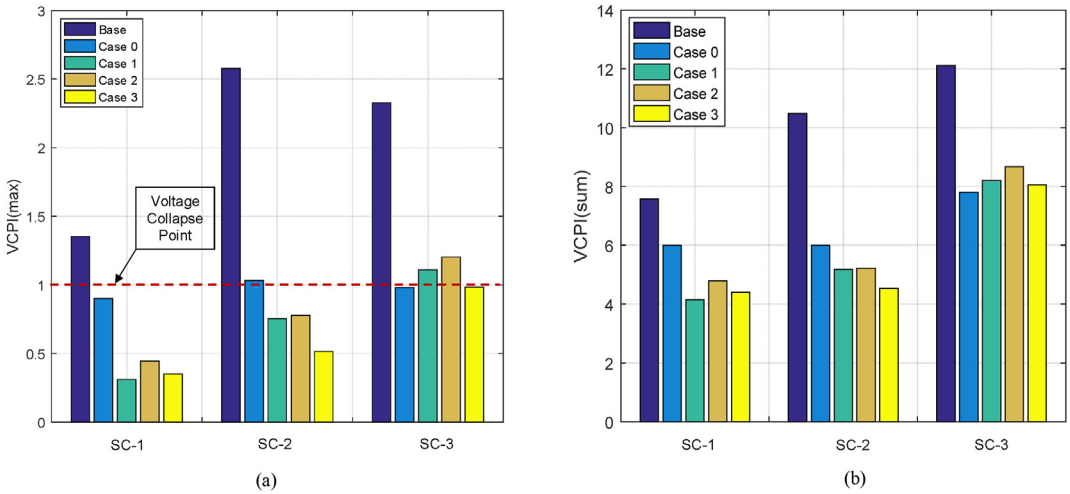

Figure 17. IEEE 30-bus voltage stability performance for different scenarios by: (a) VCPI(max) (b)VCPI(sum).

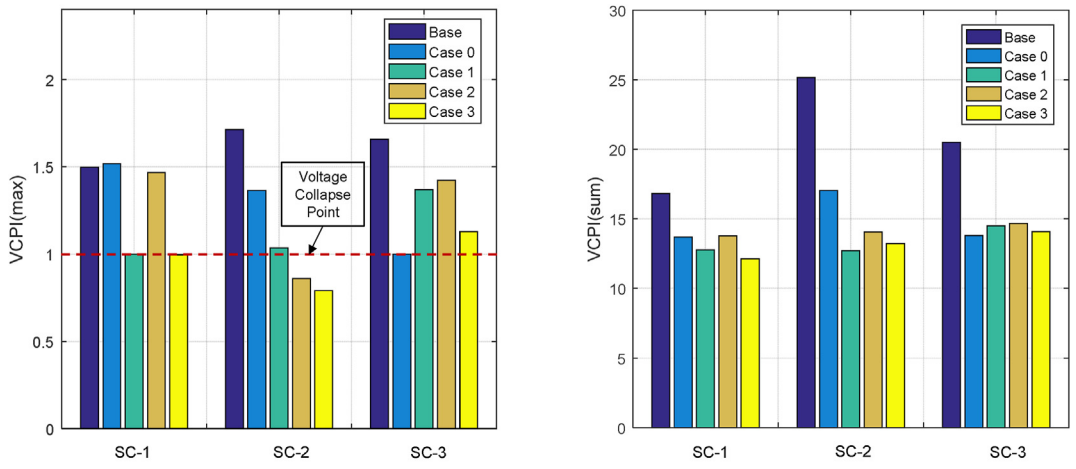

Figure 18. IEEE 57-bus voltage stability performance for different scenarios by: (a) VCPI(max) (b)VCPI(sum).

4.3.3. Minimization of the VCPI index

As discussed in sections 4.1 and 4.2, Figures 17 and 18 summarize the achieved voltage stability margin improvement by minimizing the Voltage Collapse Proximity Index. The figures show that the multi-objective optimization (Case 3) achieves the biggest VCPI improvement of 74.1% and 80.01% during normal and contingency conditions for the IEEE 30-bus. However, the single objective optimization (Case 0) alone can achieve the desired system voltage stability level during stressed conditions, improving it by 57.79%, in comparison to the base case. Similar improvement is achieved in the IEEE 57-bus, with Case 3 indicating VCPI reduction of up to 33.52% and 53.72% during normal and line outage conditions. Case 0 still achieves the most voltage stability improvement of 39.71% in stressed conditions.

5. Conclusion

In this paper, a multiobjective voltage stability-constrained optimal power flow is presented. The approach proposed incorporated the Voltage Collapse Proximity Index (VCPI) in the conventional OPF problem to enhance the static voltage stability margin while simultaneously reducing system losses and generation cost. Minimization of generation cost, transmission power loss, and line VCPI are used to develop the multiobjective functions. Lower index values indicate greater improvements in voltage stability.

The standard IEEE 30-bus and 57-bus systems were employed to investigate the impact of different operating scenarios on the control variables. The Preference Selection Index indicated that the multi-objective function of minimizing generation cost, power loss, and VCPI(max) achieved the best-optimized generation cost, power loss, and voltage stability during normal and contingency conditions. The single optimization technique proved to be the most optimal and secure way of operating the system for stressed conditions. There is a significant demand for reactive power in these conditions as the generator reactive power outputs are all maxed out. Hence, a singular focus on one objective function would be more appropriate. Therefore, it is observed that the presented multiobjective optimization control approach can be considered an effective preventive measure for normal and line outage contingency conditions, thus preventing an imminent voltage collapse. Hence, the approach can be applied in Energy Control Centres to enhance system stability and security.

However, with stressed conditions such as faults in the system, the proposed multiobjective technique faces difficulty since the system still lacks enough reactive power support. It is recommended that for future studies, incorporating Flexible AC Transmission Systems (FACTS) in the VSC-OPF can be investigated to evaluate the operational efficiency of the system.

Declarations

Author contribution statement

Rebeccah Kyomugisha: Conceived and designed the experiments; Performed the experiments; Analyzed and interpreted the data; Contributed reagents, materials, analysis tools or data; Wrote the paper.

Christopher Maina Muriithi: Conceived and designed the experiments; Analyzed and interpreted the data; Contributed reagents, materials, analysis tools or data.

Milton Edimu: Analyzed and interpreted the data; Contributed reagents, materials, analysis tools or data.

Funding statement

This work was supported by the African Union Commission.

Data availability statement

Data included in article/supp. material/referenced in article.

Declaration of interests statement

The authors declare no conflict of interest.

Additional information

No additional information is available for this paper.

References

[1] N. Thasnas, A. Siritaratiwat, Implementation of static line voltage stability indices for improved static voltage stability margin, J. Electr. Comput. Eng. 2019 (2019) 2609235.
[2] M.Z. Islam, et al., A harris hawks optimization based single- and multi-objective optimal power flow considering environmental emission, Sustainability 12 (13) (2020).
[3] S. Khunkitti, et al., A comparison of the effectiveness of voltage stability indices in an optimal power flow, IEEJ Trans. Electr. Electron. Eng. 14 (Dec. 2018).
[4] O.B. Adewuyi, H.O.R. Howlader, I.O. Olaniyi, D.A. Konneh, T. Senjyu, Comparative analysis of a new VSC-optimal power flow formulation for power system security planning, Int. Trans. Electr. Energy Syst. 30 (3) (Mar. 2020), e12250.
[5] W. Warid, Optimal power flow using the AMTPG-Jaya algorithm, Appl. Soft Comput. 91 (2020) 106252.
[6] A.A. El-Fergany, H.M. Hasanien, Salp swarm optimizer to solve optimal power flow comprising voltage stability analysis, Neural Comput. Appl. 32 (9) (2020) 5267–5283.

[7] M.-A. Nasr, S. Nikkhah, G.B. Gharehpetian, E. Nasr-Azadani, S.H. Hosseinian, A multi-objective voltage stability constrained energy management system for isolated microgrids, Int. J. Electr. Power Energy Syst. 117 (2020) 105646.

[8] K. Manoz Kumar Reddy, A. Kailasa Rao, R. Srinivas Rao, Optimal deployment of UPFC based on critical bus ranking using an effective PSO algorithm, Mater. Today Proc. (Apr. 2021).

[9] S. Nascimento, M.M. Gouvêa, Multi-objective adaptive evolutionary algorithm to enhance voltage stability in power systems, Int. J. Control. Autom. Syst. 19 (7) (Jul. 2021) 2596–2610.

[10] S. Karimulla, K. Ravi, Solving multi objective power flow problem using enhanced sine cosine algorithm, Ain Shams Eng. J. 12 (4) (2021) 3803–3817.

[11] M.Z. Islam, et al., Marine predators algorithm for solving single-objective optimal power flow, PLoS One 16 (8) (Aug. 2021), e0256050.

[12] I.H. Daghan, M.T. Gencoglu, M.T. Özdemır, Chaos embedded particle swarm optimization technique for solving optimal power flow problem, in: 2021 18th International Multi-Conference on Systems, Signals & Devices, SSD), 2021, pp. 725–731.

[13] P. Nou, Y. Zhang, Y. Yang, The impact of voltage stability constraint L-index on power system optimization base on interior point Algorithm by considering the integration of renewable energy, J. Phys. Conf. Ser. 1887 (1) (Jun. 2021) 12031.

[14] S. Duman, J. Li, L. Wu, AC optimal power flow with thermal–wind–solar–tidal systems using the symbiotic organisms search algorithm, IET Renew. Power Gener. 15 (2) (Feb. 2021) 278–296.

[15] S. Li, W. Gong, C. Hu, X. Yan, L. Wang, Q. Gu, Adaptive constraint differential evolution for optimal power flow, Energy 235 (2021) 121362.

[16] S. Gupta, N. Kumar, L. Srivastava, Bat Search Algorithm for Solving Multi-Objective Optimal Power Flow Problem BT - Applications of Computing, Automation and Wireless Systems in Electrical Engineering, 2019, pp. 347–362.

[17] A.Q. Abdulrasool, L.T. Al-Bahrani, Multi-objective constrained optimal power flow based on enhanced ant colony system Algorithm, in: 2021 12th International Symposium on Advanced Topics in Electrical Engineering, ATEE), 2021, pp. 1–5.

[18] H. Bouchekara, Solution of the optimal power flow problem considering security constraints using an improved chaotic electromagnetic field optimization algorithm, Neural Comput. Appl. 32 (7) (2020) 2683–2703.

[19] S. Gupta, N. Kumar, L. Srivastava, H. Malik, A. Anvari-Moghaddam, F.P. García Márquez, A robust optimization approach for optimal power flow solutions using rao algorithms, Energies 14 (17) (2021).

[20] S. Khunkitti, A. Siritaratiwat, S. Premrudeepreechacharn, Multi-objective optimal power flow problems based on slime mould algorithm, Sustainability 13 (13) (Jul. 2021) 7448.

[21] E. Büyük, Pareto-based multiobjective particle swarm optimization: examples in geophysical modeling, in: Swarm Intelligence [Working Title], IntechOpen, 2021.

[22] S. Khunkitti, S. Premrudeepreechacharn, Voltage stability improvement using voltage stability index optimization, in: 2020 International Conference on Power, Energy and Innovations (ICPEI), 2020, pp. 193–196.

[23] S.R. Salkuti, Optimal power flow using multi-objective glowworm swarm optimization algorithm in a wind energy integrated power system, Int. J. Green Energy 16 (15) (Dec. 2019) 1547–1561.

[24] A.-A.A. Mohamed, Y.S. Mohamed, A.A.M. El-Gaafary, A.M. Hemeida, Optimal power flow using moth swarm algorithm, Electr. Power Syst. Res. 142 (2017) 190–206.

[25] A. Khan, H. Hizam, N.I. Abdul Wahab, M.L. Othman, Solution of optimal power flow using non-dominated sorting multi objective based hybrid firefly and particle swarm optimization algorithm, Energies 13 (Aug. 2020) 4265.

[26] S. Chandrasekaran, Multiobjective optimal power flow using interior search algorithm: a case study on a real-time electrical network, Comput. Intell. 36 (Mar. 2020).

[27] C.A.C. Coello, G.T. Pulido, M.S. Lechuga, Handling multiple objectives with particle swarm optimization, IEEE Trans. Evol. Comput. 8 (3) (2004) 256–279.

[28] M.A. Abido, in: B.K. Panigrahi, Y. Shi, M.-H. Lim (Eds.), Multiobjective Particle Swarm Optimization for Optimal Power Flow Problem BT - Handbook of Swarm Intelligence: Concepts, Principles and Applications, Springer Berlin Heidelberg, Berlin, Heidelberg, 2011, pp. 241–268.

[29] S. Hemamalini, S.P. Simon, Economic/Emission Load Dispatch Using Artificial Bee Colony Algorithm, 2010.

[30] The University of Washington Electrical Engineering, Power system test case archive, the IEEE 30-bus test system data, ", https://labs.ece.uw.edu/pstca/pf30/pg_tca30bus.htm.

[31] The University of Washington Electrical Engineering, Power systems test case archive, 57 bus power flow test case. http://labs.ece.uw.edu/pstca/pf57/pg_tca57bus.htm.

[32] K. Maniya, M.G. Bhatt, A selection of material using a novel type decision-making method: Preference selection index method, Mater. Des. 31 (4) (2010) 1785–1789.

[33] J. Zhang, Q. Tang, P. Li, D. Deng, Y. Chen, A modified MOEA/D approach to the solution of multi-objective optimal power flow problem, Appl. Soft Comput. 47 (2016) 494–514.

[34] S. Kahourzade, A. Mahmoudi, H. Bin Mokhlis, A comparative study of multi-objective optimal power flow based on particle swarm, evolutionary programming, and genetic algorithm, Electr. Eng. 97 (1) (2015) 1–12.

[35] O. Herbadji, L. Slimani, T. Bouktir, Multi-objective Optimal Power Flow Considering the Fuel Cost, Emission, Voltage Deviation and Power Losses Using Multi-Objective Dragonfly Algorithm, 2017.

[36] G. Chen, J. Qian, Z. Zhang, S. Li, Application of modified pigeon-inspired optimization algorithm and constraint-objective sorting rule on multi-objective optimal power flow problem, Appl. Soft Comput. 92 (2020) 106321.

[37] M. Ghasemi, S. Ghavidel, M.M. Ghanbarian, M. Gharibzadeh, A. Azizi Vahed, Multi-objective optimal power flow considering the cost, emission, voltage deviation and power losses using multi-objective modified imperialist competitive algorithm, Energy 78 (2014) 276–289.

[38] G. Chen, X. Yi, Z. Zhang, H. Lei, Solving the multi-objective optimal power flow problem using the multi-objective firefly algorithm with a constraints-prior pareto-domination approach, Energies 11 (12) (2018).

[39] S. Gupta, L. Srivastava, Application of Multi-Objective Genetic Algorithm for Solving Optimal Power Flow Problem, Dec. 2020.

[40] M.A. Medina, S. Das, C.A. Coello Coello, J.M. Ramírez, Decomposition-based modern metaheuristic algorithms for multi-objective optimal power flow – a comparative study, Eng. Appl. Artif. Intell. 32 (2014) 10–20.

[41] B. Mahdad, K. Srairi, Security constrained optimal power flow solution using new adaptive partitioning flower pollination algorithm, Appl. Soft Comput. 46 (2016) 501–522.

[42] G. Chen, S. Qiu, Z. Zhang, Z. Sun, Quasi-oppositional cuckoo search algorithm for multi-objective optimal power flow, IAENG Int. J. Comput. Sci. 45 (May 2018) 255–266.

[43] G. Chen, J. Qian, Z. Zhang, Z. Sun, Multi-objective optimal power flow based on hybrid firefly-bat algorithm and constraints- prior object-fuzzy sorting strategy, IEEE Access 7 (2019) 139726–139745.

[44] S. Gupta, N. Kumar, L. Srivastava, H. Malik, A. Pliego Marugán, F.P. García Márquez, A hybrid jaya–powell's pattern search algorithm for multi-objective optimal power flow incorporating distributed generation, Energies 14 (10) (2021).

[45] A. Saha, P. Das, A.K. Chakraborty, Water evaporation algorithm: a new metaheuristic algorithm towards the solution of optimal power flow, Eng. Sci. Technol. an Int. J. 20 (6) (2017) 1540–1552.

[46] W. Warid, H. Hizam, N. Mariun, N.I. Abdul Wahab, A novel quasi-oppositional modified Jaya algorithm for multi-objective optimal power flow solution, Appl. Soft Comput. 65 (2018) 360–373.

[47] S.A. El-Sattar, S. Kamel, R.A. El Sehiemy, F. Jurado, J. Yu, Single- and multi-objective optimal power flow frameworks using Jaya optimization technique, Neural Comput. Appl. 31 (12) (2019) 8787–8806.